www.ietdl.org

Published in IET Microwaves, Antennas & Propagation
Received on 14th April 2011
Revised on 1st February 2012
doi: 10.1049/iet-map.2011.0459

ISSN 1751-8725

Active phase conjugation with multiple antenna array element

P. Xiao[1] *V. Fusco*[2]

[1]*Centre for Communication Systems Research, University of Surrey, Guildford, Surrey GU2 7XH, UK*
[2]*Institute of ECIT, Queen's University Belfast, Belfast BT3 9DT, UK*
E-mail: v.fusco@ecit.qub.ac.uk

Abstract: In this study, the authors analyse the temporal and spatial compression characteristics of retrodirective antenna systems wherein active phase conjugation (APC) is deployed. It is shown that under the APC Hermitian channel matrix properties result and these lead to opportunities for both temporal and spatial signal compression. The effects of additive channel noise, as well as compression assistance given by multipath richness are described. Some general properties of retrodirective antenna systems with respect to linear and circular polarised pilot signals are also discussed. The scheme elaborated here is compliant with a generic channel model and can therefore be easily incorporated into any readily available communication systems analysis or channel modelling software. The work presented in this study provides a theoretical foundation for the previous experimental findings in APC systems.

1 Introduction

In radio or acoustic underwater communication systems a transmitted signal can follow many different propagation paths before arriving at the receiver. This causes fluctuations in the received signal's amplitude, phase and angle of arrival, and as a consequence results in multipath fading. Shallow water acoustic channels [1] and microwave radio channels in office built-up environments [2] are particularly problematic as they exhibit a large amounts of multipath interference. Various solutions have been proposed to improve communication speed and reliability in both radio and shallow water acoustic channels. Coherent receivers that use adaptive equalisation have been proposed, for example, in [3, 4] to combat the intersymbol interference (ISI) caused by frequency selective channels. Given accurate channel estimation, ISI can be effectively mitigated by the channel equalisation technique. However, a large number of taps are usually required by the equalisers for dispersive channels and these taps must be constantly adjusted to compensate for the changing environment, resulting in a substantial computational burden.

The phase conjugation technique can be used in order to avoid explicit channel estimation and subsequent equalisation by implicitly recombining the multipath arrival signals, [5–8]. This technique can be categorised into active phase conjugation (APC) [5, 6] and passive phase conjugation (PPC) [7, 8] approaches.

Antenna arrays are individual radiating elements combined so that they function and perform like a single large antenna. Retrodirective antenna arrays, as the name suggests, have a special feature. When receiving a signal from an unspecified direction, the array can automatically transmit a signal response to that same direction without any previous knowledge of the source direction [6, 9, 10]. This effect is made to occur automatically by sampling the incoming wavefront, and applying the APC technique. Since the phase of the incident signal is now phase conjugated, the signal retransmitted from the array will self-steer along the direction of the incident wavefront back to the spatial position of the originating pilot tone [11]. The overall system behaves as a directional antenna with omni-directional coverage and allows tracking of fast-moving targets. A related application of this technology is the automotive collision avoidance system, which provides the services of warning a driver of potential hazards in his path, including vehicles and roadside obstacles. As illustrated in Fig. 1, vehicle radars first emit modulated continuous waves or pulse waves and receive echoes from other vehicles or roadside obstacles, for example, man-made traffic structures, topographic structures and so on. Information such as distance and speed can then be determined from the echoes to generate warning signals. Retrodirective arrays need to be placed on the vehicle surfaces and road obstacles for the system to work efficiently. Other applications of retrodirective array include tracking of low-earth orbiting satellites, terrestrial mobile communications and so on.

2 Active phase conjugation analysis

Fig. 2 illustrates the principle of APC. The channel impulse response function is $h(t)$ and its Fourier transform is $H(f)$; the transmitted signal is $s(t)$ and its Fourier transform is

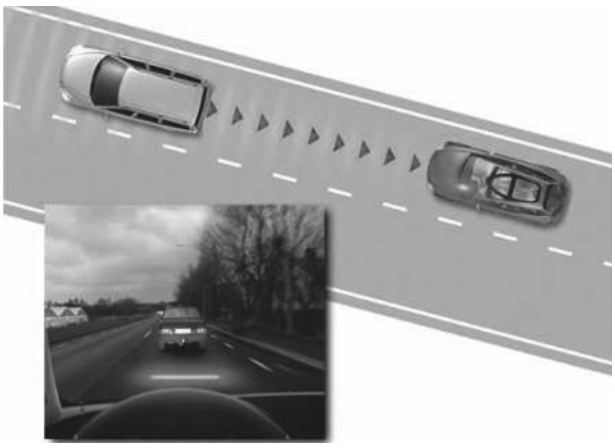

Fig. 1 *Illustration of an automotive collision avoidance system which warns the driver a potential collision*

The radar system installed in the red car first sends an interrogating signal (an interrogating signal is used by an electronic device to detect the presence of surrounding objects, to estimate their distances and moving speeds) indicated by the yellow beams, the retrodirective array mounted on the grey car upon receiving the signal, applies the principle of APC, that is, phase conjugates the signal, and retransmits this signal back to the red car to track the grey car's distance, speed and so on. and generate warning if necessary. When the warning signal is generated, the driver will see the flashing lights reflected in the windshield

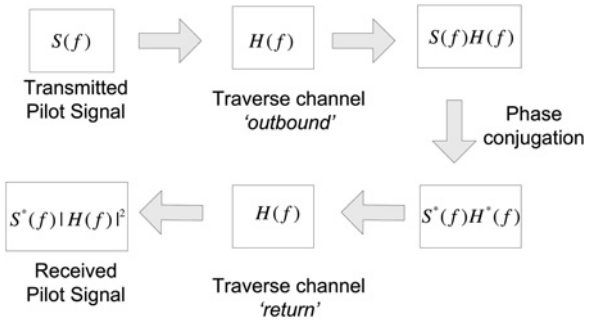

Fig. 2 *Active Phase conjugation*

$S(f)$. The APC scheme operates as follows: the transmitter sends a signal $S(f)$, which traverses the channel $H(f)$, and is observed by the receiver as $S(f)H(f)$; the receiver phase conjugates the signal, producing $S^*(f)H^*(f)$, and retransmits the signal back to the transmitter. Assuming that the channel is quasi-stationary and remains static during the return transmission, the signal $S^*(f)H^*(f)$ travels back through the same channel, resulting in $S^*(f)|H(f)|^2$ at the transmitter. Consequently, the received signal is a scaled version of the conjugate of the transmitted signal. In this way, it reconcentrates the multipath arrivals and achieves temporal compression.

In contrast with APC, the PPC procedure [8] does not require the return path retransmission. It achieves temporal compression by cross-correlating two received signals corresponding to the pilot S_1 and transmitted signal S_2.

To facilitate analysis, let us use a single-antenna APC system and a simple 3-tap sample-spaced discrete channel, shown in Fig. 3, as an example to demonstrate the effectiveness of APC in combatting the multipath effect.

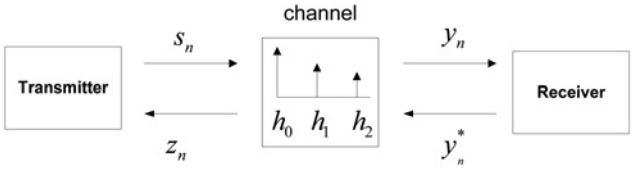

Fig. 3 *Discrete-time model for a single-antenna array APC system*

The received signal at the receiver can be expressed as

$$y_n = h_0 s_n + h_1 s_{n-1} + h_2 s_{n-2} \tag{1}$$

where h_0, h_1, h_2 are the complex channel gains for the first, second and third taps, respectively, and s_n is the transmitted symbol at the nth sample instant. The amplitude of each channel coefficient $|h_l|$, $l = 0, 1, 2$ is characterised by a Rayleigh distribution and the channel gain $|h_l|^2$ follows a χ^2 distribution with 2° of freedom. The total average channel gain $\Sigma_{l=0}^{2} E[|h_l|^2]$ is normalised to unity.

After phase conjugation and return path retransmission the signal received at the transmitter side after a round-trip through the example 3-tap system is

$$\begin{aligned} z_n &= h_0 y_{n-2}^* + h_1 y_{n-1}^* + h_2 y_n^* \\ &= R(0)s_{n-2}^* + R(1)s_{n-1}^* + R^*(1)s_{n-3}^* + R(2)s_n^* + R^*(2)s_{n-4}^* \end{aligned} \tag{2}$$

where $R(\tau)$ is the instantaneous correlation function (ICF) of the channel at the τth lag, and it depends on the instantaneous value of channel coefficients, that is

$$R(\tau) = h_i h_{i-\tau}^*$$

In the case of a 3-tap channel

$$\begin{aligned} R(0) &= |h_0|^2 + |h_1|^2 + |h_2|^2 \\ R(1) &= h_1 h_0^* + h_2 h_1^* \\ R(2) &= h_2 h_0^* \end{aligned}$$

Note that in the above derivation, the channel is assumed to be quasi-stationary such that the channel gains remain static during the forward transmission and return retransmission.

Equation (1) corresponds to the forward transmission process illustrated in upper part of Fig. 2, whereas (2) corresponds to the return path retransmission illustrated in the lower part of Fig. 2. These two equations show the time-domain convolution process between the channel and transmitted signal. According to the Fourier theorem, the time-domain convolution and time reversal, shown by (1) and (2), correponds to the frequency-domain multiplication and conjugation illustrated in Fig. 2.

From (2) and (3), it can be seen that the principle of APC operation is that it coherently reconcentrates the multipath arrivals at zeroth time lag (temporal compression). A special example is a single-tap channel, which results in a channel ICF with a strong peak at the zeroth lag and zero for all the other lags.

For an L-tap channel, (2) can be generalised to

$$\begin{aligned} z_n = {} & R(0)s_{n-L+1}^* + R(1)s_{n-L+2}^* + R^*(1)s_{n-L}^* \\ & + R(2)s_{n-L+3}^* + R^*(2)s_{n-L-1}^* + \cdots \end{aligned} \tag{3}$$

Table 1 ICF for 802.11 APC WLAN channel at 2.4 GHz (ICF = 1 at zero lag)

No. of array elements	Max magnitude of ICF sidelobe	
	11-tap channel	51-tap channel
1	0.38	0.2
10	0.07	0.05

Table 2 ICF for 802.11 APC WLAN channel at 2.4 GHz as a function of antenna correlation coefficient (ICF = 1 at zero lag)

Antenna correlation factor	Max magnitude of ICF sidelobe
0.0	0.05
0.4	0.25
0.8	0.45

It should be noted that these ICFs may also have temporal sidelobes that result in residual ISI. It is therefore desirable to reduce the sidelobes of the channel ICFs. Table 1 shows simulation results based on the IEEE 802.11 WLAN channel model [12].

The results for the number of array elements equal to 1 and 10 indicate that the 51-tap channel exhibits better correlation properties with reduced sidelobes. A rich scattering environment will reduce ISI through temporal compression because in this case, the channel coefficients appear noise-like, resulting in an ICF that has a strong peak at the zero-th lag and is nearly zero at all other lags. Thus, an APC system operating in a multipath-rich environment is expected to exhibit better ISI mitigation properties than as operating in a multipath-poor environment.

3 Analysis of multi-antenna array APC system

In this section, we analyse the APC system with antenna array. An antenna array is a set of two or more antennas, from which the signals are combined or processed in order to achieve improved performance over that of a single antenna. It is obvious to see from Table 1 that an antenna array positioned at the receiver facilitates better temporal compression since the main peaks from different elements are added coherently, whereas sidelobes are spread out because of incoherent summation of the sidelobes from different elements.

Suppose we have an N_r-element antenna array at receiver, antenna correlation factor [13] between the ith and mth elements is defined as

$$\rho_{i,m} = \left| \frac{E\{(h_i - E\{h_i\})(h_m - E\{h_m\})^*\}}{\sqrt{E\{|h_i - E\{h_i\}|^2\}E\{|h_m - E\{h_m\}|^2\}}} \right| \quad (4)$$

where h_i and h_m are the channel coefficients between the transmit antenna and the ith and mth elements of the receive antenna array, respectively. By assuming that the antenna correlation factor is identical for all elements in the array irrespective of their positions, that is, $\rho_{i,m} = \rho$ for $i = 1, \ldots, N_r$; $m = 1, \ldots, N_r$; $i \neq m$, we examine the impact of antenna correlations on channel ICF in Table 2. Here the slidelobes of the channel ICF become larger as the correlation factor ρ increases. Thus, antenna correlations adversely affect the ICF of the channel and diminish sidelobe averaging effects.

In the multi-antenna array APC system shown in Fig. 4, the transmitter has 2×1 array elements and the receiver has $M \times N$ array elements. An array of $M \times N$ elements is defined as a spatially extended collection of $M \times N$ similar radiators, having the same polar radiation patterns and the same orientation in 3D space. The system has two pilot sources which transmit pilots S_1 and S_2 from the 2×1 array elements to which the $M \times N$ phase conjugate array will self steer the return signal to. These pilot signals can be transmitted with either vertical (horizontal) linear polarisation or circular polarisation depending on the application, for example, linear polarisation for terrestrial mobile communications, and circular polarisation for ground-to-satellite communications. The task is to obtain the signals at their originating positions after a round trip through the system. The multipath channel contains direct and indirect paths because of scatterers. In the channel the signal experiences time delay and phase shift, as well as attenuation of amplitude because of free-space path loss. The received signals are locally phase conjugated and retransmitted through the same element. We assume that the channel has rich scattering properties, thus based on our findings in Section 2, ISI effects can be neglected. The received signal at $N_r = M \times N$ array elements can be approximated as

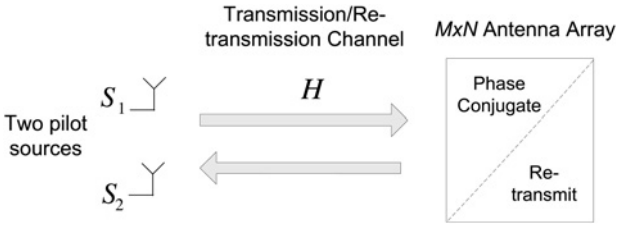

Fig. 4 *Multi-antenna array APC system under investigation*
The pilot sources are the transmit array elements which are used to transmit pilot signals

$$\underbrace{\begin{bmatrix} Y_1 \\ Y_2 \\ \vdots \\ Y_{N_r} \end{bmatrix}}_{Y} \simeq \underbrace{\begin{bmatrix} H_{11} & H_{12} \\ H_{21} & H_{22} \\ \vdots & \vdots \\ H_{N_r1} & H_{N_r2} \end{bmatrix}}_{H} \underbrace{\begin{bmatrix} S_1 \\ S_2 \end{bmatrix}}_{S} + \underbrace{\begin{bmatrix} V_1 \\ V_2 \\ \vdots \\ V_{N_r} \end{bmatrix}}_{V} \quad (5)$$

where H_{ij} is the channel coefficient between the ith receive antenna array element and the jth transmit antenna array element; V_i stands for the noise at the ith array element ($i = 1, \ldots, N_r$), it is assumed to be a complex Gaussian random variable with zero mean and variance σ_v^2, that is, $V_i \sim \mathcal{CN}(0, \sigma_v^2)$. Note that the channel matrix $\boldsymbol{H}$ in (5) would be a block toeplitz matrix in the presence of ISI [14].

The signal received at the transmitter side after a round trip through the system shown in Fig. 2 is $\boldsymbol{Z} = \boldsymbol{H}^{\mathrm{T}}\boldsymbol{Y}^*$ (where $\boldsymbol{H}^{\mathrm{T}}$

doi: 10.1049/iet-map.2011.0459

is the transposed version of $\boldsymbol{H}$), that is

$$\underbrace{\begin{bmatrix} Z_1 \\ Z_2 \end{bmatrix}}_{\boldsymbol{Z}} = \underbrace{\begin{bmatrix} H_{11} & H_{21} & \dots & H_{N_r 1} \\ H_{12} & H_{22} & \dots & H_{N_r 2} \end{bmatrix}}_{\boldsymbol{H}^{\mathrm{T}}} \times \left(\underbrace{\begin{bmatrix} H_{11}^* & H_{12}^* \\ H_{21}^* & H_{22}^* \\ \vdots & \vdots \\ H_{N_r 1}^* & H_{N_r 2}^* \end{bmatrix} \begin{bmatrix} S_1^* \\ S_2^* \end{bmatrix} + \begin{bmatrix} V_1^* \\ V_2^* \\ \vdots \\ V_{N_r}^* \end{bmatrix}}_{\boldsymbol{Y}^*} \right)$$

$$= \underbrace{\begin{bmatrix} \sum_{i=1}^{N_r} |H_{i1}|^2 & \sum_{i=1}^{N_r} H_{i1} H_{i2}^* \\ \sum_{i=1}^{N_r} H_{i1}^* H_{i2} & \sum_{i=1}^{N_r} |H_{i2}|^2 \end{bmatrix}}_{\boldsymbol{R}} \begin{bmatrix} S_1^* \\ S_2^* \end{bmatrix} + \begin{bmatrix} \sum_{i=1}^{N_r} H_{i1} V_i^* \\ \sum_{i=1}^{N_r} H_{i2} V_i^* \end{bmatrix} \tag{6}$$

The matrix $\boldsymbol{R}$ is formed as $\boldsymbol{R} = \boldsymbol{H}^{\mathrm{T}} \boldsymbol{H}^*$, its off-diagonal elements are

$$R_{12} = \sum_{i=1}^{N_r} H_{i1} H_{i2}^*$$

$$R_{21} = \sum_{i=1}^{N_r} H_{i1}^* H_{i2}$$

Obviously, $\boldsymbol{R}$ is a Hermitian matrix since $R_{ij} = R_{ji}^*$. Transmit diversity is a radio communication technique using signals that originate from two or more independent sources that have been modulated with identical information-bearing signals and that may vary in their transmission characteristics at any given instant. It can help overcome the effects of fading, and circuit failures. In order to achieve transmit diversity we transmit the same pilot signal from the transmit antenna array elements (e.g., $S_1 = S_2 = S$, i.e. linear polarisation), then combine the returned signals at transmitter, resulting in

$$Z = Z_1 + Z_2 = \left[\sum_{i=1}^{N_r} (|H_{i1}|^2 + |H_{i2}|^2) + 2 \left\{ \sum_{i=1}^{N_r} H_{i1} H_{i2}^* \right\} \right] \times S^* + \sum_{i=1}^{N_r} (H_{i1} + H_{i2}) V_i^* \tag{7}$$

Equation (7) shows that each frequency component of the return signal Z is a scaled and conjugate version of the originally transmitted signal S (corrupted with additive noise), which is true regardless of antenna polarisation. This follows from the fact that for a Hermitian matrix, addition of its off-diagonal elements results in a real-valued scaling factor, no signal rotations are incurred. It is also obvious to see from (7) that the retrodirective array has the capability of redirecting energy back along incoming multipaths such that they will coherently combine at the original source location. This proves our previous experimental finding reported in [10].

Equations (6) and (7) also hold for APC systems with antenna correlations (mutual couplings) since antenna correlations do not change the fact that the matrix $\boldsymbol{R}$ is Hermitian. However, antenna correlations do affect the ICF of the channel and act to diminish the sidelobe averaging effects as discussed in the previous section. Therefore it is desirable to design systems with low antenna correlations.

Next we derive expressions of the received signal for the following special scenarios:

1. Assume $N_r = M \times N = 2$ and that the transmitter has only one antenna, $S_1 = S_2 = S$ (linear polarisation), we obtain

$$Z = Z_1 + Z_2 = \left[\sum_{i=1}^{2} (|H_{i1}|^2 + |H_{i2}|^2) + 2 \left\{ \sum_{i=1}^{2} H_{i1} H_{i2}^* \right\} \right] \times S^* + \sum_{i=1}^{2} (H_{i1} + H_{i2}) V_i^* \tag{8}$$

Since $H_{11} = H_{12} = H_1$ and $H_{21} = H_{22} = H_2$ thus

$$Z = 2[|H_1|^2 + |H_2|^2] S^* + 2[H_1 V_1^* + H_2 V_2^*] \tag{9}$$

The received signal is a scaled and conjugated version of the transmitted signal plus additive noise.

2. If $S_1 = S\mathrm{e}^{\mathrm{j}\alpha}$ is oriented along the horizontal axis and $S_2 = S\mathrm{e}^{\mathrm{j}\alpha \pm \pi 2}$ is oriented along the vertical axis (α is an arbitrary phase shift), then from (6) we conclude that a transmitted circularly polarised signal will be received with the same hand of polarisation but with its phase conjugated.

4 Spatial reception properties

Now we investigate the scenario when a signal after a round trip transmission through the system is received not only by the two antennas that originally transmit pilots S_1 and S_2, but also by two other antennas located at different spatial positions. This scenario arises when the special focusing properties of the APC arrangement are to be evaluated. By using different receive antennas at different spatial locations we provide a means by which we can sample the region surrounding the antennas that originally transmit pilots. In this case, (6) can be reformed as

$$\boldsymbol{Z} = \begin{bmatrix} \boldsymbol{H}^{\mathrm{T}} \\ \boldsymbol{G}^{\mathrm{T}} \end{bmatrix} \boldsymbol{Y}^* = \begin{bmatrix} \boldsymbol{H}^{\mathrm{T}} \boldsymbol{Y}^* \\ \boldsymbol{G}^{\mathrm{T}} \boldsymbol{Y}^* \end{bmatrix} = \begin{bmatrix} \boldsymbol{H}^{\mathrm{T}} \boldsymbol{H}^* \boldsymbol{S}^* + \boldsymbol{H}^{\mathrm{T}} \boldsymbol{V}^* \\ \boldsymbol{G}^{\mathrm{T}} \boldsymbol{H}^* \boldsymbol{S}^* + \boldsymbol{G}^{\mathrm{T}} \boldsymbol{V}^* \end{bmatrix} \tag{10}$$

where the vector $\boldsymbol{Z}$ is re-defined as $\begin{bmatrix} Z_1 & Z_2 & Z_3 & Z_4 \end{bmatrix}^{\mathrm{T}}$; G_{ij} is the channel coefficient between the jth ($j = 3,4$) antenna at the transmitter side and the ith antenna at the receiver side, and

$$\boldsymbol{G}^{\mathrm{T}} = \begin{bmatrix} G_{13} & G_{23} & \dots & G_{N_r 3} \\ G_{14} & G_{24} & \dots & G_{N_r 4} \end{bmatrix};$$

$$\boldsymbol{Y}^* = \underbrace{\begin{bmatrix} H_{11}^* & H_{12}^* \\ H_{21}^* & H_{22}^* \\ \vdots & \vdots \\ H_{N_r 1}^* & H_{N_r 2}^* \end{bmatrix}}_{\boldsymbol{H}^*} \underbrace{\begin{bmatrix} S_1^* \\ S_2^* \end{bmatrix}}_{\boldsymbol{S}^*} + \underbrace{\begin{bmatrix} V_1^* \\ V_2^* \\ \vdots \\ V_{N_r}^* \end{bmatrix}}_{\boldsymbol{V}^*} \tag{11}$$

In (10), $\boldsymbol{R} = \boldsymbol{H}^{\mathrm{T}} \boldsymbol{H}^*$ is a Hermitian matrix, whereas this is not true for $\boldsymbol{G}^{\mathrm{T}} \boldsymbol{H}^*$. The conclusion is that the signal received at the

first two antennas that transmit S_1 and S_2 exhibit the special compression properties discussed earlier. However, for signals received at the other two antennas at different spatial locations, effective high-quality compression will not occur. Consequently, at positions more remote from the original source positions, recovery of data becomes increasingly more difficult, this was demonstrated experimentally in [10].

5 Simulation results

Simulation results are shown in this section for the system analysed in Section 3. The system has two pilot sources transmitting pilots S_1 and S_2, which are 90° phase-rotated version of each other, and each represents a block of 200 QPSK symbols. These symbol sets are transmitted over 11-path 802.11 WLAN channels and the results are averaged over 3000 channel and noise realisations.

The effect of additive noise is examined in Fig. 5, where we see the performance of APC as a function of signal to noise ratio (SNR) defined by E_b/N_0 in the dB scale, the number of array elements is set to be $N = 20$. A 20-element phase-conjugating array represents a typical scenario that could be realised from a practical perspective, such that a well collimated return signal to the pilot tone location will occur. If more sources (pilots at the same frequency) are added, their effect is simply to cause the signal returned from the phase-conjugating array to be shared out to each of the pilot tone locations. Since these systems are designed to provide high-precision retrodirective action on a single carrier we have selected two sources, nominally collocated, in order to investigate the main properties of the system for single-carrier tracking under different polarisation states.

The following seven different receiver schemes have been tested:

- Scheme 1: only Z_1 in (6) is used to decode the transmitted symbols.
- Scheme 2: only Z_2 in (6) is used to decode the transmitted symbols.
- Scheme 3: only Z_3 in (10) is used to decode the transmitted symbols.
- Scheme 4: only Z_4 in (10) is used to decode the transmitted symbols.
- Scheme 5: Both Z_1 and Z_2 are used to decode the transmitted symbols. Since the 90° phase shift between S_1 and S_2, the received signal is combined such that $Z = Z_1 - jZ_2$.
- Scheme 6: Z_1, Z_2, Z_3, Z_4 are all used to decode the transmitted symbols, the signal is combined such that $Z = Z_1 - jZ_2 + Z_3 - jZ_4$.
- Scheme 7: Z_3, Z_4 are used to decode the transmitted symbols, the signal is combined such that $Z = Z_3 - jZ_4$.

One can see from Fig. 5 that Scheme 5 achieves the best performance compared to all the other schemes because of the diversity gain obtained by combining Z_1 and Z_2. The APC system cannot operate with Scheme 3 and 4 because $\boldsymbol{G}^{\mathrm{T}}\boldsymbol{H}^{*}$ in (10) is no longer Hermitian, and consequently the compression effect is not guaranteed. On the contrary, the use of Z_3 and Z_4 serves as an additional source of noise because of the randomness of $\boldsymbol{G}^{\mathrm{T}}\boldsymbol{H}^{*}$, thus degrades system performance. Scheme 6 exploits the diversity gain by coherently combining Z_1 and Z_2, however, it also suffers from additional noise because of Z_3 and Z_4. Therefore it exhibits a worse performance than Scheme 5. Schemes 1 and 2 have almost the identical performance, but both are inferior to Scheme 5 owing to the lack of diversity gain. In all the investigated scenarios, noise has an adverse effect on the system performance, thus a reasonable level of SNR needs to be maintained for the proper functioning of APC. For example, if an APC system under Scheme 5 has a target bit error rate of 10^{-3}, it has to operate in an environment where the SNR has to be greater than 8.4 dB.

In Fig. 6, we show the performance of APC as a function of the number of array elements N_{r} for the various schemes mentioned above. Here the SNR value is fixed at $E_b/N_0 = 12$ dB. For Schemes 1, 2, 5, 6, the system performance improves as the number of array elements increases, especially for Scheme 5 with diversity exploited in the decoding process. As analysed earlier, better correlation property and thus better compression can be achieved by increasing N_{r}, leading to better BER performance, as verifed in Fig. 6.

In Fig. 7, we show the performance of APC as a function of SNR for different values of N_{r} under Scheme 5. The employed 11-path WLAN channel is by itself sufficiently rich in scattering such that the BER floor at high SNR does not occur even when a very small number of array elements are employed at the receiver, for example, when $N_{\mathrm{r}} = 5$. The

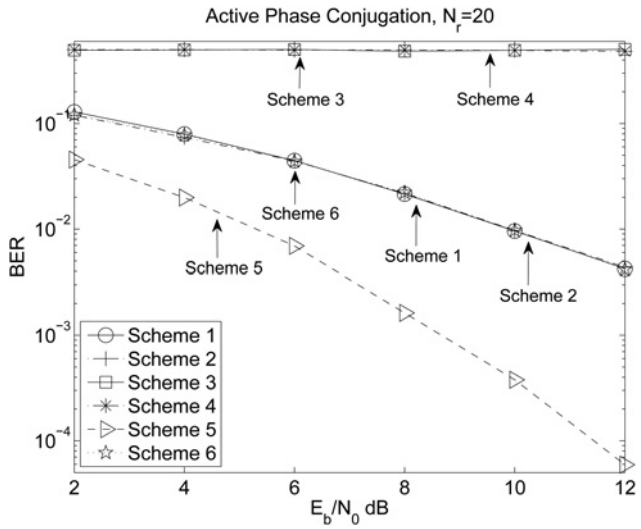

Fig. 5 *Performance of APC as a function of SNR for 11-tap WLAN channel, $N_r = 20$*

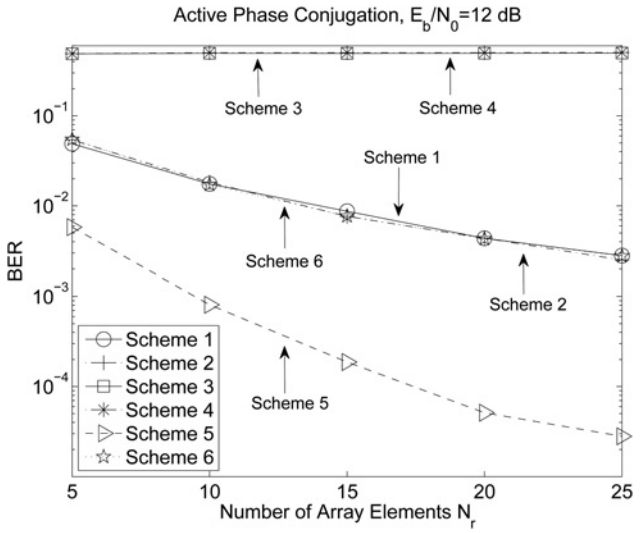

Fig. 6 *Performance of APC as a function of N_r for 11-tap WLAN channel*

doi: 10.1049/iet-map.2011.0459

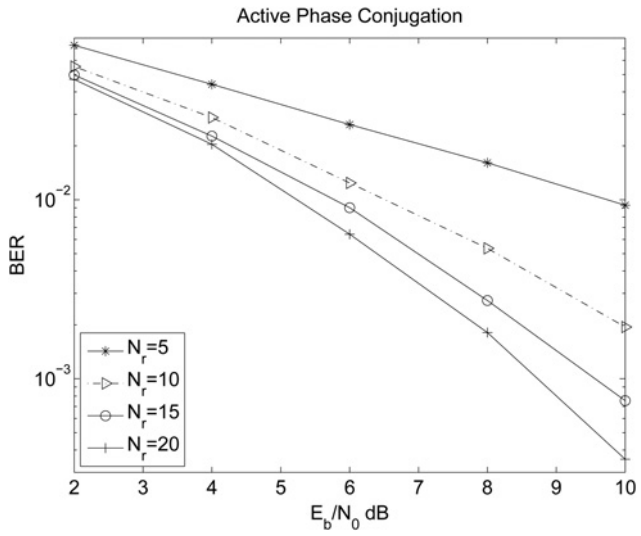

Fig. 7 *Performance of APC (Scheme 5) as a function of SNR for 11-tap WLAN channel, $N_r = 5, 10, 15, 20$*

most noticeable gain is observed when increasing N_r from 5 to 10, after which point performance gain gradually becomes saturated as the number of array elements is further increased.

In Fig. 8, we show the performance of APC as a function of the number of array elements N_r for different levels of SNR under Scheme 5. In harsh channels with high noise level, for example, when $E_b/N_0 = 4$ dB, the system performance cannot be significantly improved by inceasing N_r since noise is the dominant factor. The gain achieved by increasing N_r is more obvious at high SNRs, for example, when $E_b/N_0 = 13$ dB, since noise becomes less dominant, and ISI plays the more important role in system performance. The SNR level needs to be reasonably large in order for the multi-array APC system to be beneficial. In this case, a larger number of array elements will achieve better compression, thus less ISI and better BER performance.

In Fig. 9, we examine the impact of antenna correlations on the performance of APC. Here we assume that the correlation factor ρ (a scalar between 0 and 1) is identical for all antennas in the array irrespective of their positions. Fig. 9 indicates that the performance of the APC system with Schemes 1 and 5 becomes worse as the channels become more correlated

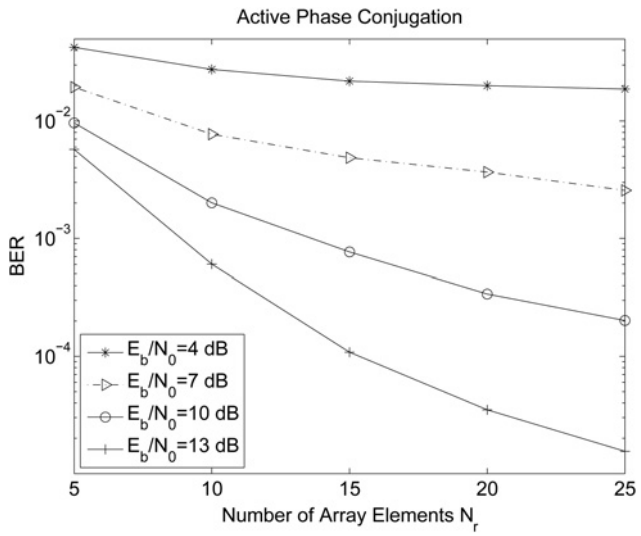

Fig. 8 *Performance of APC (Scheme 5) as a function of N_r for 11-tap WLAN channel*

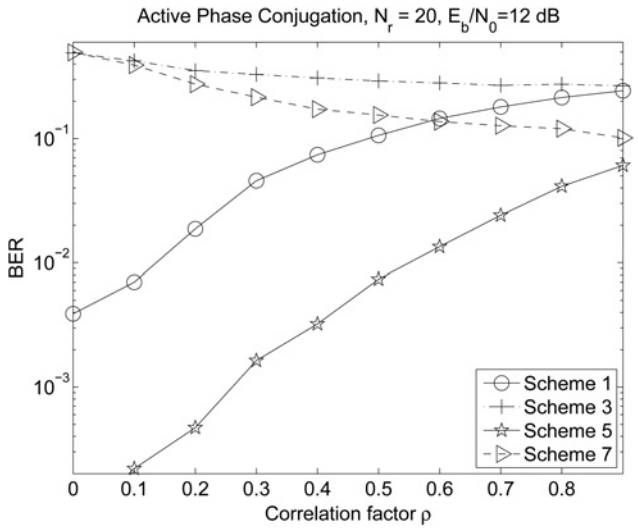

Fig. 9 *Impact of antenna correlations on the performance of APC*

(ρ increases). As analysed in Section 1, antenna correlations adversely affect the ICF of the channel and diminish sidelobe averaging effects. However, when decoded with Z_3 (Scheme 3), the system performance improves marginally as ρ increases. This follows from the fact that when the $\boldsymbol{G}$ matrix in (10) is more correlated to the $\boldsymbol{H}$ matrix as is the case when ρ increases, $\boldsymbol{G}^{\mathrm{T}}\boldsymbol{H}^{*}$ starts to resemble a Hermitian matrix, and thus the compression effect is achieved to a certain degree. This effect is more obvious when both Z_3 and Z_4 are used for symbol decoding (Scheme 7) as indicated by the figure, again reinforcing our earlier comments on spatial and temporal compression.

6 Conclusions

The temporal and spatial compression characteristics of retrodirective antenna systems with multiple antenna array elements have been discussed in this paper. It has been shown by using a discrete time channel transfer function model that Hermitian matrix properties result under the APC channel and that this leads to opportunities for both temporal and spatial signal compression. Simulations based on QPSK transmission in conjunction with an 802.11 wireless propagation model are used to demonstrate these effects. The theoretical framework developed in this paper enables us to verify some properties of APC systems with respect to linearly and circularly polarised signals. For example, a transmitted linearly/circularly polarised signal will be received with the same kind of polarisation but with its phase conjugated.

7 Acknowledgments

The work was carried out under the support of the UK Engineering and Physical Science Research Council (EPSRC) under grant EP01707X/1 and the Northern Ireland Department of Education and Learning Strengthening All Island Scheme, Mobile Wireless Futures Programme.

8 References

1 Yi, T., Xu, X.: 'Simulation study of multi-path characteristics of acoustic propagation in shallow water wireless channel'. Int. Conf. on Wireless Communication, Networking and Mobile Computing, 2007, pp. 1068–1070

2 Boyer, P.: 'Performance based on selective multipath reception', *IEEE Trans. Commun.*, 2004, **52**, (2), pp. 280–288

3 Stojanovic, M., Catipovic, J., Proakis, J.: 'Phase-coherent digital communications for underwater acoustic channels', *IEEE J. Ocean. Eng.*, 1994, **19**, pp. 100–111
4 Stojanovic, M.: 'Recent advances in high-speed underwater acoustic communication', *IEEE J. Ocean. Eng.*, 1996, **21**, pp. 125–136
5 Jackson, D., Dowling, D.: 'Phase-conjugation in underwater acoustics', *J. Acoust. Soc. Am.*, 1991, **95**, (3), pp. 1450–1458
6 Toh, B.Y., Fusco, V.F., Buchanan, N.B.: 'Assessment of performance limitations of PON retrodirective arrays', *IEEE Trans. Antennas Propag.*, 2002, **50**, (10), pp. 1425–1432
7 Rouseff, D., Jackson, D., Fox, W., Jones, C., Ritcey, J., Dowling, D.: 'Underwater acoustic communication by passive-phase conjugation: theory and experimental results', *IEEE J. Ocean. Eng.*, 2001, **26**, (4), pp. 821–831
8 Hursky, P., Porter, M., Siderius, M.: 'Point-to-point underwater acoustic communications using spread-spectrum passive phase conjugate', *J. Acoust. Soc. Am.*, 2006, **120**, (1), pp. 247–257
9 Leong, K., Miyamoto, R., Itoh, T.: 'Moving forward in retrodirective antenna array', *IEEE Potentials*, 2003, **22**, (3), pp. 16–21
10 Buchanan, N.B., Fusco, V.F.: 'Bit error rate performance enhancement of a retrodirective array over a conventional fixed beam array in a dynamic multipath environment', *IEEE Trans. Antennas Propag.*, 2010, **58**, (4), pp. 757–762
11 Pon, C.Y.: 'Retrodirective array using the heterodyne technqiue', *IEEE Trans. Antennas Propag.*, 1964, **AP-12**, (2), pp. 176–180
12 O'Hara, B., Petrick, A.: 'IEEE 802.11 handbook: a designer's companion' (IEEE, 2005, 2nd edn.)
13 Ozdemir, M.K., Arvas, E.: 'Dynamics of spatial correlation and implications on MIMO systems'. IEEE MTT-S Int. Microwave Symp., 2005, pp. 1723–1726
14 Barbero, L., Xiao, P., Ratnarahah, T., Sellathurai, M., Cowan, C.: 'A sphere decoder with approximate QR decomposition for frequency-selective channels'. Proc. IEEE Int. Conf. on Communications, May 2010

doi: 10.1049/iet-map.2011.0459